

**The following resources related to this article are available online at [www.sciencemag.org](http://www.sciencemag.org) (this information is current as of November 15, 2009):**

**Updated information and services**, including high-resolution figures, can be found in the online version of this article at:

<http://www.sciencemag.org/cgi/content/full/306/5704/2068>

**Supporting Online Material** can be found at:

<http://www.sciencemag.org/cgi/content/full/306/5704/2068/DC1>

A list of selected additional articles on the Science Web sites **related to this article** can be found at:

<http://www.sciencemag.org/cgi/content/full/306/5704/2068#related-content>

This article **cites 30 articles**, 9 of which can be accessed for free:

<http://www.sciencemag.org/cgi/content/full/306/5704/2068#otherarticles>

This article has been **cited by** 128 article(s) on the ISI Web of Science.

This article has been **cited by** 20 articles hosted by HighWire Press; see:

<http://www.sciencemag.org/cgi/content/full/306/5704/2068#otherarticles>

This article appears in the following **subject collections**:

Chemistry

<http://www.sciencemag.org/cgi/collection/chemistry>

Information about obtaining **reprints** of this article or about obtaining **permission to reproduce this article** in whole or in part can be found at:

<http://www.sciencemag.org/about/permissions.dtl>

width to below 100 Hz (24). Similarly, a larger signal can be obtained by using a laser with a higher repetition rate; for example, a 1-GHz laser with the same average power and spectral width could increase the signal up to a 100-fold (25). One practical consequence of these results is a method to control both degrees of freedom of the femtosecond comb directly by an optical transition in cold atoms. Another interesting application of the demonstrated pulse accumulation effect is laser cooling of atoms that require coherent ultraviolet light not easily accessible by conventional laser sources (26). For general coherent control experiments, pulse accumulation (when enabled by long coherence times) can complement spectral amplitude and phase manipulations, leading to improved efficiency in population control with the added spectral resolution due to multipulse interference. The precise and phase-coherent pulse accumulation may prove particularly useful in efficiently populating atomic Rydberg states for quantum information processing. Although the current experiment involves two-photon transitions, the

advantages of DFCS should apply equally to single-photon and multiphoton excitations. Multiple ultrafast lasers with optical spectra independently tailored for different spectroscopic features could be phase coherently stitched together (27, 28) to further extend the utility of this approach.

## References and Notes

1. T. C. Weinacht, J. Ahn, P. H. Bucksbaum, *Nature* **397**, 233 (1999).
2. A. H. Zewail, *Angew. Chem. Int. Ed.* **39**, 2587 (2000).
3. T. Udem, J. Reichert, R. Holzwarth, T. W. Hänsch, *Opt. Lett.* **24**, 881 (1999).
4. T. Udem, J. Reichert, R. Holzwarth, T. W. Hänsch, *Phys. Rev. Lett.* **82**, 3568 (1999).
5. L. S. Chen, J. Ye, *Chem. Phys. Lett.* **381**, 777 (2003).
6. S. A. Diddams *et al.*, *Science* **293**, 825 (2001).
7. J. Ye, L. S. Ma, J. L. Hall, *Phys. Rev. Lett.* **87**, 270801 (2001).
8. G. Wilpers *et al.*, *Phys. Rev. Lett.* **89**, 230801 (2002).
9. S. T. Cundiff, J. Ye, *Rev. Mod. Phys.* **75**, 325 (2003).
10. T. H. Yoon, A. Marian, J. L. Hall, J. Ye, *Phys. Rev. A* **63**, 011402 (2000).
11. D. J. Jones *et al.*, *Science* **288**, 635 (2000).
12. N. Dudovich, B. Dayan, S. M. G. Faeder, Y. Silberberg, *Phys. Rev. Lett.* **86**, 47 (2001).
13. J. E. Bjorkholm, P. F. Liao, *Phys. Rev. Lett.* **33**, 128 (1974).
14. O. Poulsen, N. I. Winstrup, *Phys. Rev. Lett.* **47**, 1522 (1981).

15. R. Teets, J. Eckstein, T. W. Hänsch, *Phys. Rev. Lett.* **38**, 760 (1977).
16. M. J. Snadden, A. S. Bell, E. Riis, A. I. Ferguson, *Opt. Commun.* **125**, 70 (1996).
17. D. Felinto, C. A. C. Bosco, L. H. Acioli, S. S. Vianna, *Opt. Commun.* **215**, 69 (2003).
18. D. Felinto, L. H. Acioli, S. S. Vianna, *Phys. Rev. A* **70**, 043403 (2004).
19. R. G. Brewer, E. L. Hahn, *Phys. Rev. A* **11**, 1641 (1975).
20. F. Nez, F. Biraben, R. Felder, Y. Millerieux, *Opt. Commun.* **102**, 432 (1993).
21. J. Ye, S. Swartz, P. Jungner, J. L. Hall, *Opt. Lett.* **21**, 1280 (1996).
22. G. P. Barwood, P. Gill, W. R. C. Rowley, *Appl. Phys. B* **53**, 142 (1991).
23. A. Marian, M. C. Stowe, J. Ye, in preparation.
24. R. J. Jones, I. Thomann, J. Ye, *Phys. Rev. A* **69**, 051803 (2004).
25. N. V. Vitanov, P. L. Knight, *Phys. Rev. A* **52**, 2245 (1995).
26. D. Kielpinski, <http://arxiv.org/abs/quant-ph/0306099> (2003).
27. R. K. Shelton *et al.*, *Science* **293**, 1286 (2001).
28. K. W. Holman, D. J. Jones, J. Ye, E. P. Ippen, *Opt. Lett.* **28**, 2405 (2003).
29. We are indebted to X.-Y. Xu, T. H. Yoon, L. S. Ma, T. M. Fortier, J. L. Hall, D. J. Jones, and E. Arimondo for their technical help and discussions during various stages of this work. The work at JILA is supported by the Office of Naval Research, NASA, NIST, and NSF.

24 September 2004; accepted 8 November 2004

Published online 18 November 2004;

10.1126/science.1105660

Include this information when citing this paper.

# REPORTS

## Building Programmable Jigsaw Puzzles with RNA

Arkadiusz Chworos,<sup>1</sup> Isil Severcan,<sup>1</sup> Alexey Y. Koyfman,<sup>1,2</sup>  
Patrick Weinkam,<sup>1,4</sup> Emin Oroudjev,<sup>3</sup> Helen G. Hansma,<sup>3</sup>  
Luc Jaeger<sup>1,2\*</sup>

One challenge in supramolecular chemistry is the design of versatile, self-assembling building blocks to attain total control of arrangement of matter at a molecular level. We have achieved reliable prediction and design of the three-dimensional structure of artificial RNA building blocks to generate molecular jigsaw puzzle units called tectosquares. They can be programmed with control over their geometry, topology, directionality, and addressability to algorithmically self-assemble into a variety of complex nanoscopic fabrics with predefined periodic and aperiodic patterns and finite dimensions. This work emphasizes the modular and hierarchical characteristics of RNA by showing that small RNA structural motifs can code the precise topology of large molecular architectures. It demonstrates that fully addressable materials based on RNA can be synthesized and provides insights into self-assembly processes involving large populations of RNA molecules.

DNA has been extensively used to generate artificial geometrical objects like polyhedra (1–3), various self-assembling two-dimensional (2D) nanostructures (4, 5–6), and DNA nanomechanical devices (7–9). Seeman, Winfree, and collaborators (1, 4, 5) have shown that DNA tiles based on various “crossover” DNA motifs could assem-

ble in a predictable manner into periodic and aperiodic patterned 2D arrays. These DNA arrays are still made of a limited number of distinct molecular tiles and display rather simple patterning with no finite dimensions. However, their work suggests that versatile programmable molecular systems capable of algorithmic assembly into an

infinite variety of 2D or three-dimensional (3D) supra-architectures with increasing pattern complexity, shape, molecular diversity, and size could potentially be generated with nucleic acids (10).

Although more chemically labile than DNA, natural RNAs offer a richer treasure trove of rigid structural motifs (11–14) that can be potential modules for supramolecular engineering (15–20). RNA tectonics (15) refers to the modular character of RNA, which can be decomposed and reassembled to create new RNA nanoscopic architectures. With the idea in mind to generate addressable materials with increasing patterns of complexity and molecular diversity, we have used a sequential stepwise assembly strategy to construct programmable building blocks with RNA tectonics. These molecules behave as “smart” RNA pieces, which could ultimately self-assemble in a predictable manner into any possible 2D architecture with full control over size, shape, and pattern geometry. Thus, the final position of each molecule can eventually be known and, therefore, be addressable, within a molecular jigsaw puzzle of finite size.

At a molecular level, “square-shaped” RNA supramolecules with sticky, interacting tails can potentially be programmed to assemble into many different planar networks of predefined geometries. We chose

two small RNA structural motifs present in the ribosome crystallographic structures (12–14) to guide our design of a self-assembling square made of four similar but nonidentical subunits, called tectoRNAs (Fig. 1, A and B) (21). Each tectoRNA contains two interacting hairpin loops (19, 22) covalently joined by a small structural motif of 11 nucleotides, called the right angle (RA) motif, that specifies 90° angle corners between adjacent helices within the context of the ribosome (12, 13). To avoid homomultimers, the formation of a closed, circular tetramer is directed by four distinct, specific noncovalent loop-loop interactions, called kissing loop (KL) complexes (22), which are expected to adopt collinear extended helical structures according to the crystallographic structures of the ribosome (12) and the dimerization initiation site of human immunodeficiency virus (HIV) RNA (22). A tectosquare 3D model resembles a square when viewed from the top. Nevertheless, it is not flat, because its extended helical sides adopt a log cabin-like conformation at the level of RA corners (Fig. 1C; fig. S1). Rather than being a perfect four-fold pseudosymmetrical object ( $C_4$ ), the tetramer has two-fold pseudosymmetry ( $C_2$ ). Small (ST) and large (LT) tectosquares, with 10-nm and 13-nm side lengths, can be constructed from tectoRNAs with hairpin stems of 9 and 15 base pairs (bp), respectively.

Tectosquares can further self-assemble through specific sticky tail connectors (Fig. 1). The tails of the tectoRNAs can be designed to have a wide variety of sequences. Their precise positioning and orientation are inferred from the RA motif geometry. The 3' tail, stacked in continuity to the 3' stem-loop, is expected to be structurally more constrained and directional than the 5' tail. By swapping the RA motif, the orientation of the 3' tail can be modified by 90° without changing the overall positioning of the stem-loop arms (Fig. 1D). Moreover, small variations in the tail length can change the overall length of tail connectors by one-half of a helical turn, which positions two adjacent tectosquares in either a cis or trans configuration (Fig. 1E). About 88.5 million distinct tectosquares can be built with a limited set of 12 tail connectors with two different tail orientations and sizes (23).

We constructed two sets of tectoRNAs for building ST and LT tectosquares (21).

<sup>1</sup>Department of Chemistry and Biochemistry, <sup>2</sup>Biomolecular Science and Engineering Program, <sup>3</sup>Department of Physics, University of California, Santa Barbara, CA 93106–9510, USA. <sup>4</sup>Department of Chemistry and Biochemistry, University of California, San Diego, CA 92093, USA.

\*To whom correspondence should be addressed. E-mail: jaeger@chem.ucsb.edu

Each tectoRNA sequence was optimized to favor folding into a unique, stable secondary structure (17, 24). After being synthesized by run-off transcription, tectosquare modular assembly was monitored by native polyacrylamide gel electrophoresis (PAGE). Magnesium is absolutely required for assembly.

At 0.2 mM  $Mg(OAc)_2$ , an equimolar mixture of each tectoRNA set forms 60 to 90% of a circular supramolecular species that migrates slower than monomers and linear tetramers lacking one of the four KL motifs (Fig. 2A). Remarkably, both tectosquares can be purified out of native PAGE

**Fig. 1.** Tectosquare structure and assembly principles. (A) Assembly scheme. (B) TectoRNA 2D diagram: LT tectoRNAs have stems 6 bp longer than ST tectoRNAs. N, nt positions involved in stems; x and X, nt from the 3' tail (in red) and KL loops (in green and blue) involved in Watson-Crick bp for tail-connectors or KL motif formation, respectively. RA motif consensus sequence is in orange. (C) Tectosquare 3D model (LT). Front and side views are shown. KL loops form four sequence-specific KL motifs (in blue, red, magenta, and green) that adopt collinear topologies (see also fig. S1). (D) Change of 3' tail directionality upon RA motif swapping. (E) Tectosquare cis and trans assembly configurations. (F) The five types of tectosquares used in this study.

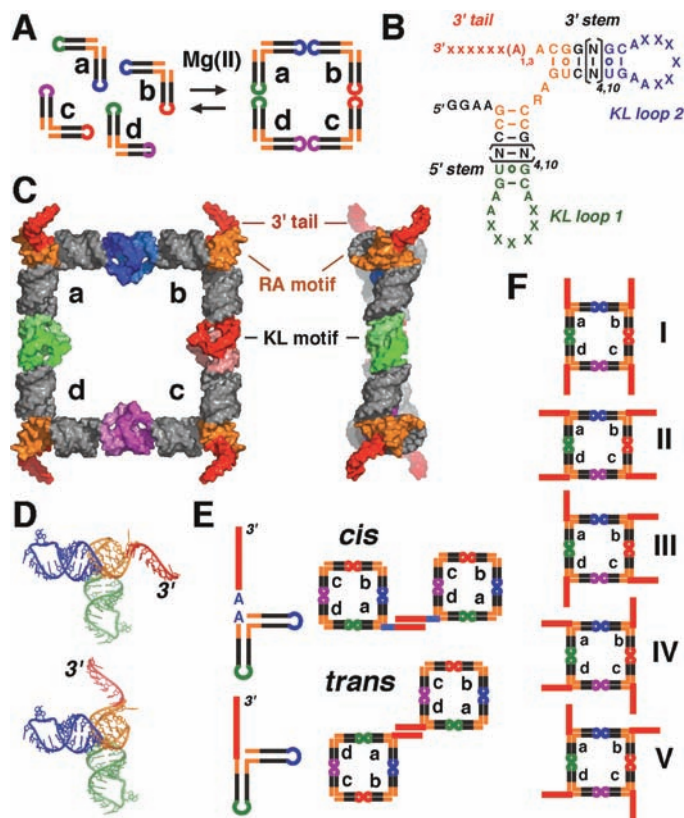
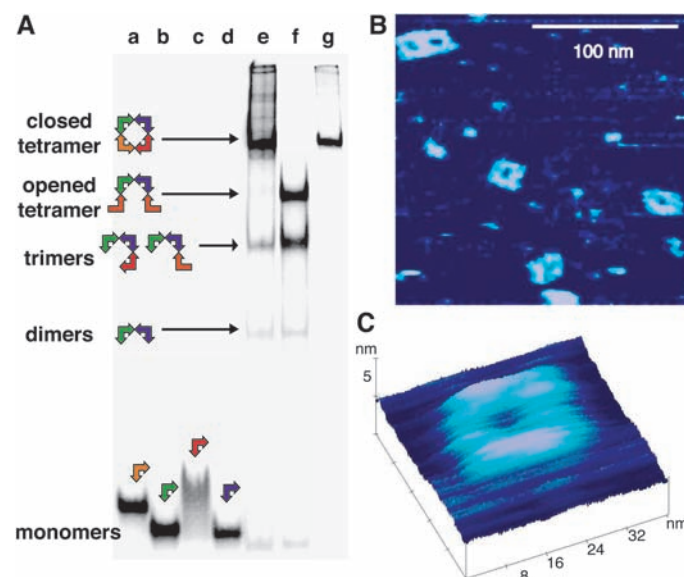


**Fig. 2.** RNA tectosquares are stable and stiff supramolecular assemblies. (A) Nondenaturing PAGE at 0.2 mM  $Mg(OAc)_2$  of various combinations of LT tectoRNAs. Lanes a, b, c, and d: tectoRNAs, a, b, c, and d, respectively, at a final concentration of 20 nM. Lane e: equimolar mixture of a, b, c, and d (20 nM each). Lane f: equimolar mixture of tectoRNAs a, b, e, and f (20 nM each). Units e and f assemble with a and b, respectively, but prevent the formation of a circular complex. Lane g: tectosquare after nondenaturing PAGE gel purification and elution at 4°C in the presence of 15 mM  $Mg(OAc)_2$ . Tectosquares can be kept at 4°C for several days without showing any sign of dissociation or degradation. (B and C) AFM visualization of LT tectosquare in solution on mica surface (B) or in air after precipitation of the RNA on mica coated with poly-L-lysine (C).



gels without dissociating (Fig. 2). We investigated further tectosquare stability by temperature-gradient gel electrophoresis (fig. S2), a method for separating different assemblies on the basis of temperature-dependent conformational change (25). In 15 mM Mg<sup>2+</sup>, tectosquares are stable up to 56°C because of the presence of the two structural motifs encoded within their sequence. With equilibrium constants of dissociation ( $K_d$ ) ranging from 1 to 20 nM at 0.2 mM Mg<sup>2+</sup>, KL motifs are more stable than RNA duplexes of identical sequences (19, 26). Moreover, tectosquares that contain the RA motif in each of their units are 4.2°C (ST) to 5.8°C (LT) more stable than those without any RA motif (fig. S2). Accordingly, the thermal stability of a tectosquare increases with an increasing number of RA motifs present within its assembly.

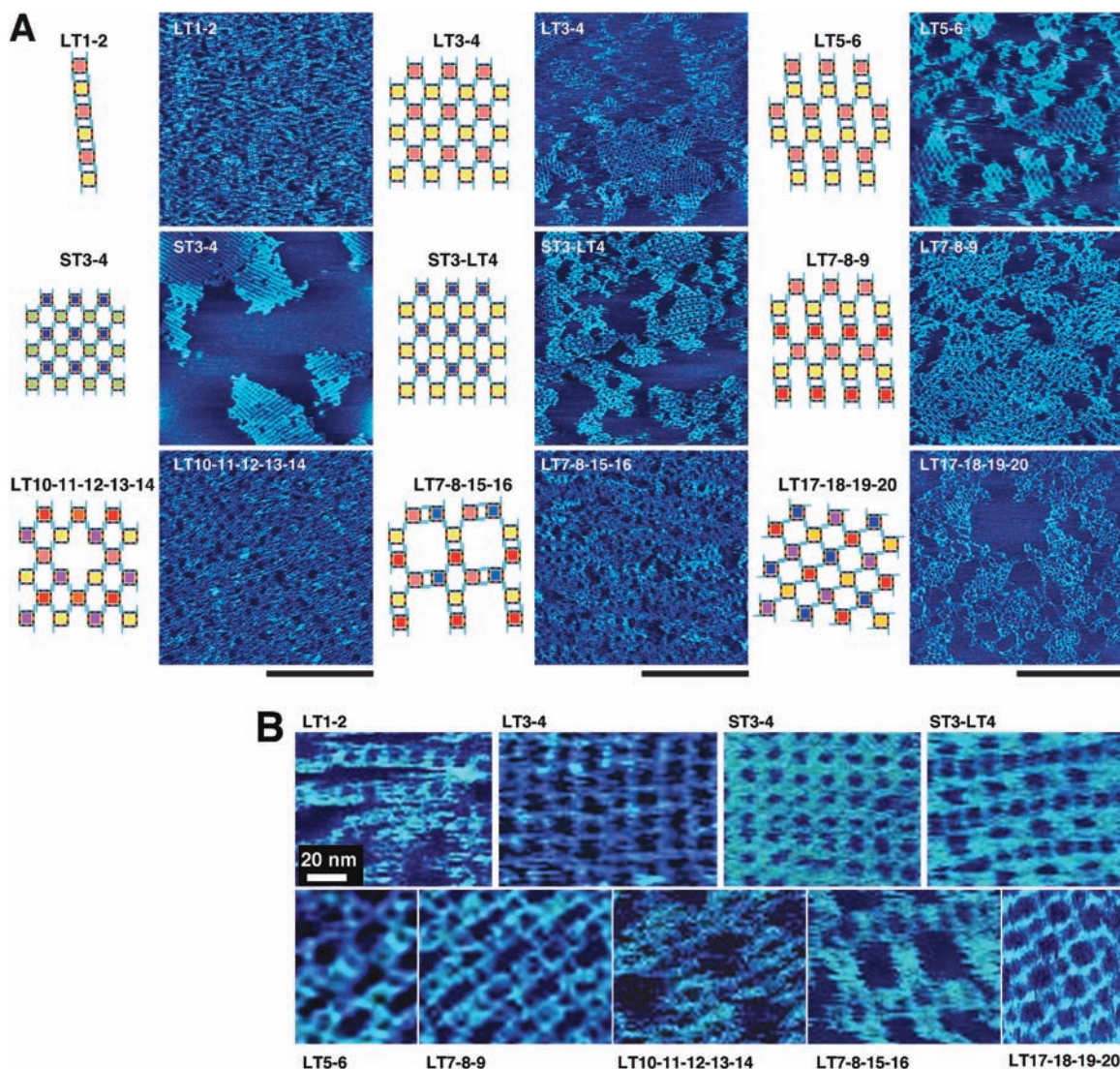
The overall topology of an LT was investigated by atomic force microscopy (AFM) (21, 27) in air or in 15 mM Mg(OAc)<sub>2</sub>

solution after deposition of the RNA sample on a mica surface. The predicted and observed tectosquare architectures (Fig. 2, B and C) are in remarkable agreement with each other and unambiguously establish the RA and KL motifs as autonomous folding modules outside their natural context. The LT folds into a square shape with stiff, straight sides of  $13 \pm 3$  nm and corners between 70° and 110°. The central cavity has an overall size of  $8 \pm 3$  nm, and the width of the RNA helical region is estimated to be  $3 \pm 1$  nm at half height, the expected width for a double-stranded RNA helix. The seldom-observed rhombus shape for LT is indicative of a tilted rather than flat tetramer that could be deformed when forced to lie on the mica surface.

The stable, rigid characteristics of tectosquares are particularly attractive for building programmable planar supra-architectures. To demonstrate the predicted geometrical properties of tectosquares described above (Fig. 1), we designed 12 specific 3' tail

connectors of 6 bp and used them to program the assembly of nine different sets of tectosquares into distinctive periodic fabrics (Fig. 3A). The connectors have similar free energies of formation, chosen to be less stable by at least two orders of magnitude than those of KL complexes. At 15 mM Mg<sup>2+</sup>, two tectosquares joined by two parallel tail connectors disassemble around 30°C; that is, 25°C below tectosquare melting temperature. A simple monitoring of the RNA annealing temperature can thus be used to hierarchically control the assembly process by uncoupling tectosquare association from fabric formation. Forty-nine tectoRNAs with different sizes, tail sequences, tail lengths, and orientations were synthesized and combined to separately construct a total of 22 tectosquares that were then appropriately mixed to generate the nine tectosquare patterns. Pattern formation was performed at 15 mM Mg<sup>2+</sup>, on the mica surface, by slow cooling from 50° to 4°C and was monitored by AFM under

**Fig. 3.** Diagram and AFM images of tectosquare nanopatterns generated from 22 tectosquares. (A) One micrometer square scale AFM images obtained in solution for: LT1-2, ladder pattern; LT3-4, fish net pattern; LT5-6, diamond pattern; ST3-4, striped velvet pattern; ST3-LT4, basket weave pattern; LT7-8-9, lace pattern; LT10-11-12-13-14, polka dot pattern; LT7-8-15-16, tartan pattern; LT17-18-19-20, cross pattern. Scale bars, 500 nm. (B) Magnification of patterns in (A). Scale bar, 20 nm. (See also fig. S3.)



aqueous conditions, similar to those used for native PAGE.

We first designed two distinct pairs of large tectosquares, LT1-2 and LT3-4, characterized by the same four tail-connector sequences oriented parallel to “a-d” and “b-c” (LT type I, Fig. 1F), but with tails of 12 and 10 nucleotides, respectively. LT1-2, with connectors of length equivalent to 14 bp, adopts a cis configuration (Fig. 1E) that leads to ladders of 10 to 20 LT (Fig. 3 and fig. S3). By contrast, LT3-4, with connectors of length equivalent to 10 bp, assembles in a trans configuration and forms fish net-like 2D lattices involving up to 100 LTs. In the ladder and 2D lattice arrangements, each LT contacts two and four other LTs, respectively (Fig. 3 and fig. S3). The next set, LT5-6, presents a combination of two of the previous pairs of long and short connectors. This molecular arrangement leads to the formation of stable tectosquare dimers assembling into diamond-like arrays that are as large as LT3-4 arrays but with meshes twice as big ( $14 \pm 2$  nm by  $27 \pm 3$  nm) (Fig. 3). STs efficiently assemble into predetermined architectures as well. The ST3-4 pair, with the same connectors as LT3-4, forms large arrays that can span almost 1  $\mu$ m and can involve more than 500 tectosquares. The plain central cavity of ST3 and ST4, too small to be well resolved by AFM, gives a striped velvet texture to these assemblies (Fig. 3; fig. S3). STs and LTs can also be combined when in the trans configuration. For example, the mix of ST3 and LT4 forms basket weave patterns characteristic of the LT and ST alternating arrangement (Fig. 3).

More complex patterns can be obtained from a greater number of tectosquares by using additional tail connectors or by preventing association at specific positions within the 2D lattice. Both LT7-8-9 and

LT10-11-12-13-14 sets take advantage of six connectors to form the lace and polka dot patterns, respectively (Fig. 3 and fig. S3). For LT10-11-12-13-14, the regularly spaced dotted motif is programmed with five LTs assembling symmetrically in an all trans configuration network, two of them lacking one of their tails.

Tectosquare assembly is highly dependent on the directionality of the 3' tail (Fig. 1F). We observed significantly larger architectures with type I LT networks than with type II (fig. S4, A and B) (28). Nevertheless, patterns taking advantage of eight connectors with various 3' tail orientations can be obtained. The tartan pattern LT7-8-15-16 is derived from the lace pattern LT7-8-9 (Fig. 3A), by replacement of LT9 with LT15-16, a tectosquare dimer formed by association of type III and type IV LTs (Fig. 1F). The different directionality of LT15 and LT16 tails leads to the formation of a lattice with meshes of  $28 \pm 3$  nm, twice as big as those obtained with LT5-6 and LT7-8-9 (Fig. 3B). LT17-18-19-20, a set of four type V tectosquares with 3' tails pointing in the four cardinal directions, assembles into the cross pattern corresponding to a  $C_4$  pseudosymmetrical arrangement of LTs (Fig. 3A). This regular lattice has two distinct square-shaped mesh sizes of  $12 \pm 2$  nm and  $17 \pm 2$  nm that correspond to the LT structure and the central hole formed by association of four LTs, respectively (Fig. 3B).

As an initial step toward fully addressable self-assembling materials, we designed three sets of tectosquares to assemble specifically into finite aperiodic nanogrids (Fig. 4; fig. S4). To control the size and shape of the RNA assembly, some LTs lacking a 3' tail at specific corners are programmed to act as edges. The 2 by 2 grid is a cross of 45 nm formed of four type V LTs linked by four

different connectors. The 3 by 3 and 4 by 4 grids are symmetrical, modular arrangements of five and eight different type I LTs, respectively. In the 3 by 3 grid, four edge LTs are linked to a central LT by six different connectors. In the 4 by 4 grid, six edge LTs assemble around a central 2 by 2 cross of two LTs through 12 different connectors. According to our structural models, the 2 by 2 grid is not perfectly flat. This partially explains its infrequent observation on the mica surface and the rhombus, rather than square, shape adopted by the 2 by 2 LT during the AFM imaging process (Fig. 4). By contrast, more than a hundred diamond-shaped 3 by 3 grids are identified on a  $16\text{-}\mu\text{m}^2$  surface, in perfect agreement with the flat planar arrangement expected for type I LTs (Fig. 4; fig. S4, C and D). The 4 by 4 grid demonstrates that the assembly of up to 27 different tectoRNAs can be hierarchically and reproducibly controlled to form RNA nanoscale jigsaw puzzles, which suggests that aperiodic assemblies of even greater molecular diversity can be obtained with additional connectors (29).

We have demonstrated that two rRNA structural motifs participate in a predictable manner to stabilize, position, and pack RNA helices without the need of proteins. The length and geometry, rather than the sequence of loops, predispose the formation of linear coaxial stacks of helices in KL complexes. Similarly, it is the bent geometry of the RA motif that favors stacking of the 3' end tail connector in continuity with its 3' stem. The importance of base stacking is emphasized by the inability of unstacked dangling 5' tail connectors to form any organized networks. Thus, in both the ribosome and tectosquares, RA and KL motifs are likely to assist the assembly process not only by local contributions to a specific RNA fold but also by reducing the entropy cost.

The subtle interplay of enthalpy and entropy that successfully promotes the formation of tectosquare assemblies is highly dependent on the strength, length, and orientation of the tail connectors and the environmental cues (RNA and divalent ion concentrations, temperature, and assembly protocols). For instance, thermodynamically stronger tail connectors of the same order of magnitude as KL complexes, as well as a reduced initial temperature of assembly, can negatively contribute to ordered assembly by kinetically trapping tectosquares in wrong configurations. Moreover, variation of the magnesium concentration can be used to switch on and off tectosquare assembly. Understanding phase diagrams for assembly is thus important for finding annealing conditions to self-heal irregular lattice points. Tectosquares assemble into their respective lattices at nanomolar concentrations, where-

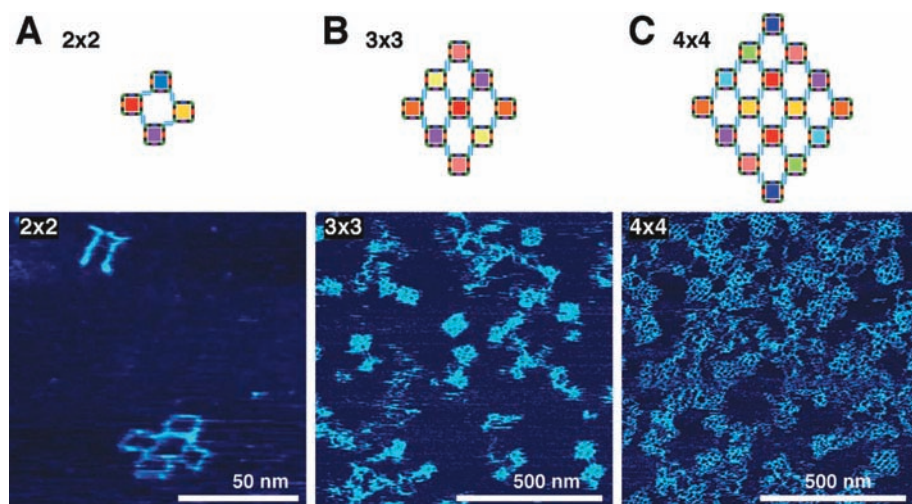


**Fig. 4.** Tectosquare nanogrids of predefined size, shape, and molecular composition. Schematic and AFM images under solution for (A) 2 by 2 (LT21-24), (B) 3 by 3 (LT10-12, 25-26), and (C) 4 by 4 (LT27-34) RNA nanogrids.

as  $K_d$  values measured for single 3' tail connectors are in the micromolar range. This fact and the small number of overlapping RNA lattices observed by AFM suggest that epitaxial phenomena occurring between RNAs and magnesium ions adsorbed on the negative mica surface might promote assembly. The observed RNA networks grow in a radial fashion. All LT tectosquare arrays involve a similar number of molecules, indicating that LT assembly is independent of the nature of the pattern formed (Fig. 3). However, STs generate significantly larger lattice networks. Despite their apparent robustness and stiffness, multiple AFM scans can disrupt the edges or deplete one or two tectosquares within the lattice. It is clear that, as a soft matter medium, the stability and size of RNA networks can still be improved and their visualization by AFM still remains challenging.

This work offers an attractive alternative to DNA, protein, and synthetic molecules for directed arrangement of matter at a molecular level (1, 30–33) and lays the foundation for generalization to periodic 3D nanomaterials of RNA. As fully addressable, programmable assemblies, tectosquare jigsaw puzzles can serve as hosts to organize at relative defined positions various molecular components with high precision and to generate nanochips, nanocircuits, and nanocrystals with potential applications in nanotechnology and material sciences (1, 32). With its underlying modular and hierarchical construction displaying a minimal set of primitive operations, the tectosquare system could possibly be a Turing-universal computing molecular system (10, 34, 35). It can also be a valuable tool for studying self-organization and emergence of complexity out of randomness (35). For instance, an unanswered question is whether combinatorial population of tectosquares could still assemble accurately into organized architectures.

#### References and Notes

- N. C. Seeman, *Nature* **421**, 427 (2003).
- W. M. Shih, J. D. Quispe, G. F. Joyce, *Nature* **427**, 618 (2004).
- C. Mao, W. Sun, N. C. Seeman, *Nature* **386**, 137 (1997).
- E. Winfree, F. Liu, L. A. Wenzler, N. C. Seeman, *Nature* **394**, 539 (1998).
- H. Yan, S. H. Park, G. Finkelstein, J. H. Reif, T. H. LaBean, *Science* **301**, 1882 (2003).
- H. Yan, T. H. LaBean, L. Feng, J. H. Reif, *Proc. Natl. Acad. Sci. U.S.A.* **100**, 8103 (2003).
- C. Mao, W. Sun, Z. Shen, N. C. Seeman, *Nature* **397**, 144 (1999).
- B. Yurke, A. J. Turberfield, A. P. Mills Jr., F. C. Simmel, J. L. Neumann, *Nature* **406**, 605 (2000).
- H. Yan, X. Zhang, Z. Shen, N. C. Seeman, *Nature* **415**, 62 (2002).
- E. Winfree, *J. Biomol. Struct. Dyn. Conversat.* **11**, 263 (2000).
- R. T. Batey, R. P. Rambo, J. A. Doudna, *Angew. Chem. Int. Ed. Engl.* **38**, 2326 (1999).
- N. Ban, P. Nissen, J. Hansen, P. B. Moore, T. A. Steitz, *Science* **289**, 905 (2000).
- B. T. Wimberly *et al.*, *Nature* **407**, 327 (2000).
- F. Schlutzen *et al.*, *Cell* **102**, 615 (2000).
- E. Westhof, B. Masquida, L. Jaeger, *Fold. Des.* **1**, R78 (1996).
- L. Jaeger, N. B. Leontis, *Angew. Chem. Int. Ed. Engl.* **39**, 2521 (2000).
- L. Jaeger, E. Westhof, N. B. Leontis, *Nucleic Acids Res.* **29**, 455 (2001).
- Y. Ikawa, K. Fukada, S. Watanabe, H. Shiraiishi, T. Inoue, *Structure (Cambridge)* **10**, 527 (2002).
- S. Horiya *et al.*, *Chem. Biol.* **10**, 645 (2003).
- B. Liu, S. Baudrey, L. Jaeger, G. C. Bazan, *J. Am. Chem. Soc.* **126**, 4076 (2004).
- Materials and methods are available as supporting material on Science Online.
- E. Ennifar, P. Walter, B. Ehresmann, C. Ehresmann, P. Dumas, *Nature Struct. Biol.* **8**, 1064 (2001).
- Considering that each of the four tectosquare units can either have no tail, or a 3' tail of  $n$  different sequences with different size ( $s$ ) and orientation ( $o$ ), a total of  $4(s+1)$  different  $a, b, c$ , and  $d$  tectoRNAs can be combined to construct  $(s+1)^4$  tectosquares.
- R. M. Dirks, M. Lin, E. Winfree, N. A. Pierce, *Nucleic Acids Res.* **32**, 1392 (2004).
- A. A. Szewczak, E. R. Podell, P. C. Bevilacqua, T. R. Cech, *Biochemistry* **37**, 11162 (1998).
- J. S. Lodmell, C. Ehresmann, B. Ehresmann, R. Marquet, *J. Mol. Biol.* **311**, 475 (2001).
- H. G. Hansma, E. Oroudjev, S. Baudrey, L. Jaeger, *J. Microsc.* **212**, 273 (2003).
- LTs associate better when tails are oriented parallel to their  $a$ - $d$  and  $b$ - $c$  sides. This fact supports our twofold symmetrical models (Fig. 1C; fig. S1), with  $a$ - $d$  and  $b$ - $c$  being parallel to each other and  $a$ - $b$  and  $c$ - $d$  being tilted. Assembly through tails oriented parallel to  $a$ - $b$  and  $c$ - $d$  is nevertheless possible.
- With 12 different tail-tail connectors, we are presently able to generate a 3 by 3 grid made of nine different tectosquares with the position of each of the 36 constitutive tectoRNAs being fully addressable within the RNA lattice.
- J. Michl, T. F. Magnera, *Proc. Natl. Acad. Sci. U.S.A.* **99**, 4788 (2002).
- N. C. Seeman, A. M. Belcher, *Proc. Natl. Acad. Sci. U.S.A.* **99** (suppl. 2), 6451 (2002).
- S. Zhang, *Nature Biotechnol.* **21**, 1171 (2003).
- P. Ringle, G. E. Schulz, *Science* **302**, 106 (2003).
- A. Carbone, N. C. Seeman, *Proc. Natl. Acad. Sci. U.S.A.* **99**, 12577 (2002).
- S. Wolfram, *A New Kind of Science* (Wolfram Media, Champaign, IL, 2002).
- This paper is dedicated to St. Joseph, patron saint of carpenters, and to F. Michel and E. Westhof, L.J.'s mentors. Thanks to S. and L. Baudrey for technical assistance and to C. Geary, H. Waite, and S. Parsons for critical reading of the manuscript. A.C. thanks the Department of Bioorganic Chemistry, Polish Academy of Sciences, CM&MS, Lodz, 90363, Poland. Funding for this work was provided by faculty start-up funds from UCSB to L.J. and by grants from NSF to L.J. (CHE-0317154 and MRSEC DMR00-80034) and H.H. (MCB0236093).

#### Supporting Online Material

www.sciencemag.org/cgi/content/full/306/5704/2068/DC1

Materials and Methods

Figs. S1 to S4

Tables S1 to S3

References and Notes

31 August 2004; accepted 8 November 2004  
10.1126/science.1104686

## Translation of DNA Signals into Polymer Assembly Instructions

Shiping Liao and Nadrian C. Seeman\*

We developed a DNA nanomechanical device that enables the positional synthesis of products whose sequences are determined by the state of the device. This machine emulates the translational capabilities of the ribosome. The device has been prototyped to make specific DNA sequences. The state of the device is established by the addition of DNA set strands. There is no transcriptional relationship between the set strands and the product strands. The device has potential applications that include designer polymer synthesis, encryption of information, and use as a variable-input device for DNA-based computation.

We built a DNA nanomechanical device that mimics the translational capabilities of the ribosome. In response to a DNA signal, it aligns a series of molecules in specific positions; these molecules are then fused together in a specific order. For convenience, we have prototyped this system with DNA, so the products are DNA oligonucleotides of a defined sequence. Thus, in this case, the chemistry of the product is similar to that of the signal molecules, but there is no complementary relationship to the signal sequences. By using DNA molecules to set the states of two DNA PX-JX<sub>2</sub> devices (1) independently, we pro-

grammed the synthesis of four different product molecules.

The PX-JX<sub>2</sub> device is a sequence-dependent DNA machine, the state of which is controlled by hybridization topology (1). It can assume two structural states (termed PX and JX<sub>2</sub>), which differ from each other by a half-turn rotation of one end of the molecule relative to the other end (Fig. 1A). Two different pairs of set strands can bind to the framework of the device, thereby establishing which structural state it adopts. The set strands contain short unpaired segments ("toeholds") at one end to facilitate their removal by unset strands that bind to the toeholds and then remove the set strands by branch migration (2). In addition to the PX-JX<sub>2</sub> device, numerous variants of sequence-dependent control, pioneered in DNA tweezers by Yurke *et al.* (2), have been reported; these include a DNA

Department of Chemistry, New York University, New York, NY 10003, USA.

\*To whom correspondence should be addressed.  
E-mail: ned.seeman@nyu.edu